

## COMPUTERIZING CALCULATIONS AND DESIGNING

### NUMERICAL MODELING SOFTWARE PACKAGE FOR COMPUTING AERODYNAMIC CHARACTERISTICS OF AIR CYCLONES

**A. V. Ivanov, G. E. Dumnov,  
A. V. Muslaev, and M. V. Popov**

*Results of numerical modeling of airflow in cyclones are presented. Calculations were made with the aid of FloEFD software package version 11.3 using a modified  $k$ - $\epsilon$  turbulence model. Calculated hydraulic resistance and cyclone separation efficiency data are compared with experimental data obtained at various inlet air temperatures in a wide airflow rate range. It was found that the used mathematical model can provide acceptably accurate results. Recommendations are offered for successful application of computational fluid dynamics (CFD) method to obtain accurate and economical cyclone aerodynamics engineering calculation results.*

**Keywords:** *cyclone, CFD, numerical modeling, hydraulic resistance, purification efficiency,  $k$ - $\epsilon$  turbulence model, swirling flow.*

Air cyclones are popular dust-catching devices used in many industrial sectors because of simple design, absence of moving parts, and low capital and operating costs, in combination with their high air purification efficiency.

In spite of the simple design and operating principle, the air motion pattern inside the cyclone is complicated because of high turbulence level, strong anisotropy, pronounced tridimensionality (3D pattern), and unsteady swirling airflow. Due to the lack of a stable theory of fluid motion in a cyclone, for new design development, one is forced to take recourse either to an empirical procedure or to a slight modification of the existing designs. Because of this, costly bench tests of prototypes are unavoidable for refining and optimizing designs.

In these situations, modeling based on computational fluid dynamics (CFD) for hydrodynamics and heat and mass transfer computation is a useful tool for calculating cyclone characteristics. CFD can be used to have a better understanding of the intricate flow field structure and to get information about the following points: hydraulic resistance of the cyclone and its dependence on specific design solutions and operating conditions; stability of the central vortex and its possible interaction with the walls of the conical part of the cyclone; quantitative and qualitative assessment of the erosional effect on the cyclone walls; the degree of air purification (cyclone efficiency).

One of the basic problems of analyzing numerical modeling results is whether they adequately portray the real picture of the physical phenomenon or of the technological process. In this work, to solve this problem, the results of numerical modeling of the key characteristics of cyclones are compared with the available experimental data.

A cylindrical air cyclone with a rectangular inlet tube for tangential gas injection was chosen as the modeling object. In this work, we describe unsteady three-dimensional (3-D) turbulent flow of viscous compressible nonuniform airflow that transports a substance (solid impurity in the form of spherical particles). The mathematical formulation of the problem

TABLE 1

$\Phi$	$\bar{\Psi}_\Phi$	$S_\Phi$
1	0	0
$\bar{U}$	$\bar{\tau}^\Sigma$	$-\nabla P' + (\rho - \rho_{\text{ref}})\bar{g}$
$H$	$\bar{U}\bar{\tau}^\Sigma + (\lambda + \lambda_t)\nabla T + \left(\mu + \frac{\mu_t}{\sigma_k}\right)\nabla k$	0
$k$	$\left(\mu + \frac{\mu_t}{\sigma_k}\right)\nabla k$	$\bar{\tau}^R\nabla(\bar{U}) - \rho\varepsilon$
$\varepsilon$	$\left(\mu + \frac{\mu_t}{\sigma_\varepsilon}\right)\nabla\varepsilon$	$f_1C_{\varepsilon 1}\frac{\varepsilon}{k}\bar{\tau}^R\nabla(\bar{U}) - f_2C_{\varepsilon 2}\frac{\rho\varepsilon^2}{k}$

includes 3-D transitional differential equations of mass conservation of turbulent airflow, its pulse and energy, and turbulence characteristics. Trajectory approach was used to simulate solid impurity transport. It is assumed that the solid impurity does not affect the flow field in the cyclone. Taking account of the familiar assumptions, the differential conservation equations system can be presented in the form

$$\frac{\partial\rho\Phi}{\partial t} + \nabla(\rho\bar{U}\Phi) = \nabla(\bar{\Psi}_\Phi) + S_\Phi, \quad (1)$$

where  $\rho$  is the air density,  $\Phi$  is the dependent variable,  $t$  is the time,  $\bar{U}$  is the velocity vector,  $\bar{\Psi}_\Phi$  is the diffusion flow, and  $S_\Phi$  is the source term.

All dependent variable and the corresponding transport coefficients and source terms are shown in Table 1.

Here

$$P' = P - P_{\text{ref}} - \rho_{\text{ref}}\bar{g}\bar{x} + \frac{2}{3}\rho k; \quad \bar{\tau}^\Sigma = (\mu + \mu_t)\bar{s}; \quad \bar{\tau}^R = \mu_t\bar{s} - \frac{2}{3}\rho kI;$$

$$\bar{s} = \nabla(\bar{U}) + (\nabla\bar{U})^T - \frac{2}{3}\nabla(\bar{U})I; \quad H = h + \frac{\bar{U}^2}{2} + \frac{5}{3}k; \quad h = c_pT; \quad \mu_t = C_\mu f_\mu \frac{\rho k^2}{\varepsilon};$$

$$f_\mu = (1 - \exp(-0.0165R_y))^2 \left(1 + \frac{7.5}{R_t}\right); \quad f_1 = 1 + \left(\frac{0.05}{f_\mu}\right)^3;$$

$$f_2 = 1 - \exp(-R_t^2); \quad R_y = \frac{\rho\sqrt{ky}}{\mu}; \quad R_t = \frac{\rho k^2}{\mu\varepsilon},$$

where  $\bar{\tau}^\Sigma$  is the total stress tensor;  $P'$  is the effective pressure;  $\rho_{\text{ref}}$  is the reference air density;  $\bar{g}$  is the free fall acceleration;  $H$  is the full specific enthalpy;  $\lambda$  is the heat conductivity coefficient;  $\lambda_t$  is the turbulent heat conductivity coefficient;  $T$  is the temperature;  $\mu$  is the dynamic molecular viscosity coefficient;  $\mu_t$  is the dynamic turbulent viscosity coefficient;  $\sigma_k$  is a constant;  $k$  is the kinetic energy of turbulent pulsations;  $\bar{\tau}^R$  is the Reynolds stress tensor;  $\varepsilon$  is the rate of dissipation of kinetic energy of turbulent pulsations;  $\sigma_\varepsilon$ ,  $C_{\varepsilon 1}$ ,  $C_{\varepsilon 2}$  are constants;  $f_1$ ,  $f_2$  are damping functions;  $P$  is the static pressure;  $P_{\text{ref}}$  is the reference pressure;  $\bar{x}$  is the radius vector;  $\bar{s}$  is the shear strain tensor;  $I$  is the unit tensor;  $h$  is the specific enthalpy;  $c_p$  is the specific heat of air;  $C_\mu$  is a constant;  $f_\mu$  is the Lam–Bremhorst damping function;  $R_y$ ,  $R_t$  are dimensionless complexes; and  $y$  is the minimum distance to the wall.

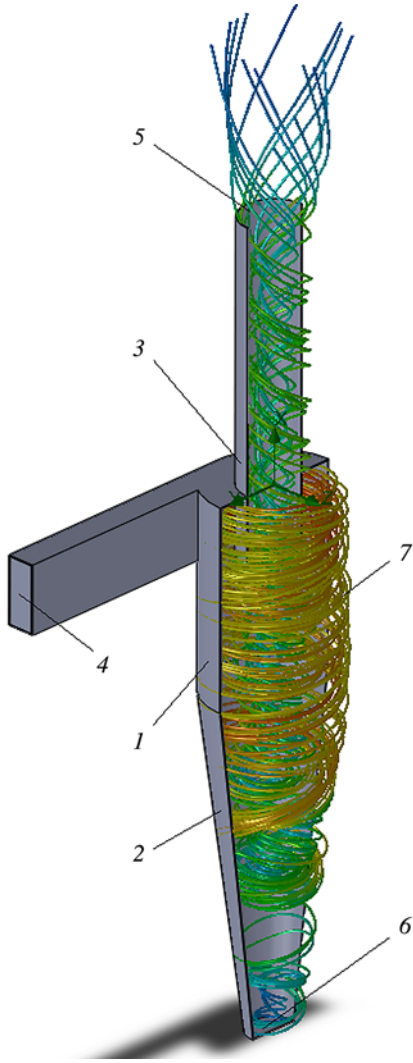


Fig. 1. Design of Stairmand HE cyclone: 1) cylindrical part; 2) conical part; 3) outlet pipe; 4) inlet pipe; 5) expulsion; 6) dust expulsion; 7) current lines.

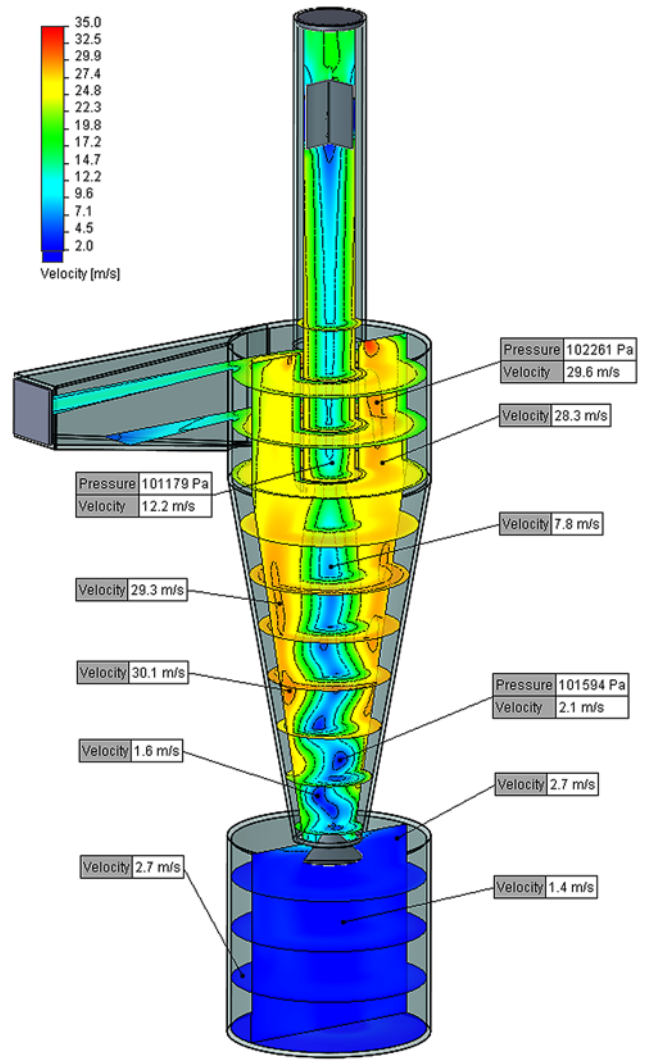


Fig. 4. Velocity distribution in cyclone.

The air density is calculated from the equation of state for an ideal gas. The dynamic molecular viscosity coefficient and air heat conductivity coefficient depend on the temperature. To close the conservation equations system, use was made of the modified Lam–Bremhorst  $k$ – $\epsilon$  turbulence model. The turbulence model constants have the following values:  $C_\mu = 0.09$ ,  $C_{\epsilon 1} = 1.44$ ,  $C_{\epsilon 2} = 1.92$ ,  $\sigma_k = 1$ , and  $\sigma_\epsilon = 1.3$  [1].

The trajectories of the solid impurity particles are determined by numerical integration of the equation

$$m_p \frac{d\vec{U}_p}{dt} = \frac{1}{8} \pi \mu d C_D (\vec{U} - \vec{U}_p) + \frac{1}{6} \pi d^3 (-\nabla P + (\rho_p - \rho) \vec{g}), \quad (2)$$

where  $m_p$  is the particle mass,  $\vec{U}_p$  is the particle velocity vector,  $d$  is the particle diameter,  $C_D$  is the particle resistance coefficient, and  $\rho_p$  is the particle density. The particle resistance coefficient was calculated by Henderson formulas [2]. The heat exchange between the particles and the gas stream was ignored. The boundary conditions for the studied modeling object include specifying the volume or mass airflow rate in the cyclone inlet tube. Zero excess pressure was assigned

TABLE 2

Geometric dimension, m	Value
Total height (cylindrical + conical parts)	1.22
Height (diameter) of cylindrical part	0.457 (0.305)
Diameter of outlet pipe	0.152
Length of upper (lower) part of outlet pipe	0.6 (0.152)
Length (width) of rectangular section of inlet pipe	0.152 (0.061)
Length of inlet pipe	0.6
Diameter of dust expulsion hole	0.114

at the outer boundaries of the calculation region for the external formulation of the problem and at the cyclone outlet pipe exit for the internal formulation of the problem. The choice of the formulation type depends on the geometry of the cyclone (examined below).

Wall functions, in conjunction with a unique model based on sub-mesh (finite-difference) resolution of the boundary layer, were used to describe viscous interaction of the turbulent airflow with the walls. This model represents a system of integral-differential equations that are solved along the wall current lines and that can be used to determine the boundary layer thickness, friction stresses, and heat flows on smooth and rough surfaces. The uniqueness of this approach is that it provides for the possibility of getting wall stresses and heat flows in the whole Reynolds number range (initial setting of the flow conditions is not compulsory) [1].

The referred system of differential conservation equations is solved numerically in a rectangular Cartesian mesh using an ambiguous finite-difference scheme and the control volume concept.

The calculations were made on a Dell PC having Precision T3500 Intel Xeon 4 CPU E5530 2.4 GHz 6.0 Gb RAM using FloEFD 11.3 software version [1]. Calculation of one version takes ~6 h. FloEFD is fully integrated in 3D solid CAD system (SolidWorks, Creo, CATIA, NX, etc.), which allows calculation of liquid and gas flows directly in the equipment development and designing environment.

To check the adequacy of mathematical modeling of the flow in the cyclone, experimental works executed in two different units were chosen [3, 4].

I. *Stairmand HE cyclone*. The geometry of the cyclone and the typical flow pattern in it are shown in Fig. 1. The key dimensions of the Stairmand HE cyclone are given in Table 2 [3].

In the experiments [3], various cyclone operation conditions were studied: mass airflow rate 0.06–0.30 kg/sec, inlet velocity 5–25 m/sec, air density  $1.29 \text{ kg/m}^3$ , and dynamic viscosity  $1.75 \cdot 10^{-5} \text{ Pa}\cdot\text{sec}$ .

The problem of calculation of flow inside the cyclone is considered in external formulation in order to avoid the need for specifying an uneven static pressure profile at the outlet pipe exit. Specifying a constant pressure at the pipe exit is improper for solving problems involving strongly swirling flows in internal formulation.

Thus, the calculation region includes the inner space of the cyclone and a part of the surrounding space. The dimensions of the modeling region are: length 0.817 m, width 0.44 m, and height 2.25 m. The particle expulsion hole was closed in both the experiment and the calculation.

For discretization of the calculation region, an unstructured rectangular Cartesian mesh adapted to a real form of bodies was used in the FloEFD package. This mesh is obtained by subdividing, in accordance with special alignments, the basic structured Cartesian mesh.

The problem was solved in unsteady-state formulation with a constant time step. The purpose of the calculations was to determine the full-pressure differential between the inlet and outlet pipes, followed by a comparison of the obtained data with the experimental ones. The sought pressure differential was averaged after this quantity attained the quasisteady state.

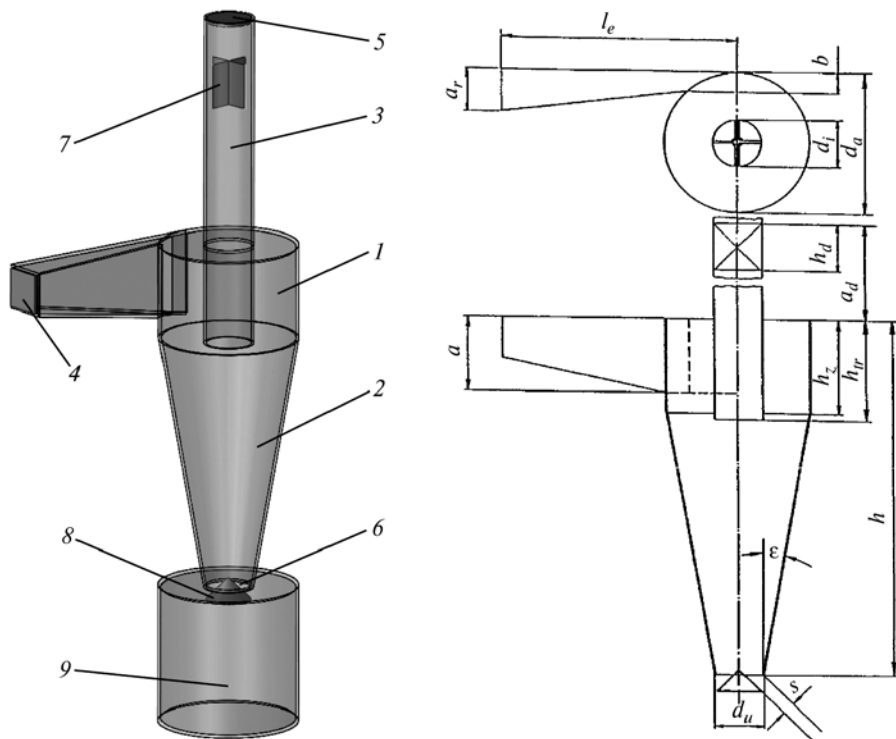


Fig. 2. Design of cyclone with bin: see Fig. 1 for numbers 1–6; 7) flow straightening device; 8) deflecting cone; 9) dust bin.

TABLE 3

Geometric dimension	Value
Diameter of cylindrical part $d_a$ , m	0.15
Diameter of outlet pipe $d_i$ , m	0.05
Diameter of dust expulsion hole $d_u$ , m	0.05
Cyclone height $h$ , m	0.387
Inlet pipe length $l_e$ , m	0.245
Inlet pipe height at cyclone entrance $a$ , m	0.02
Inlet pipe width at cyclone entrance $b$ , m	0.08
Height of cylindrical part $h_z$ , m	0.104
Length of lower part of outlet pipe $h_{lr}$ , m	0.11
Length of upper part of outlet pipe $a_d$ , m	0.21
Height of flow straightening device $h_d$ , m	0.05
Length of side of tetragonal section of inlet pipe $a_r$ , m	0.044
Clearance width $s$ , m	0.01
Tilt angle $\epsilon$ of conical part, deg	10

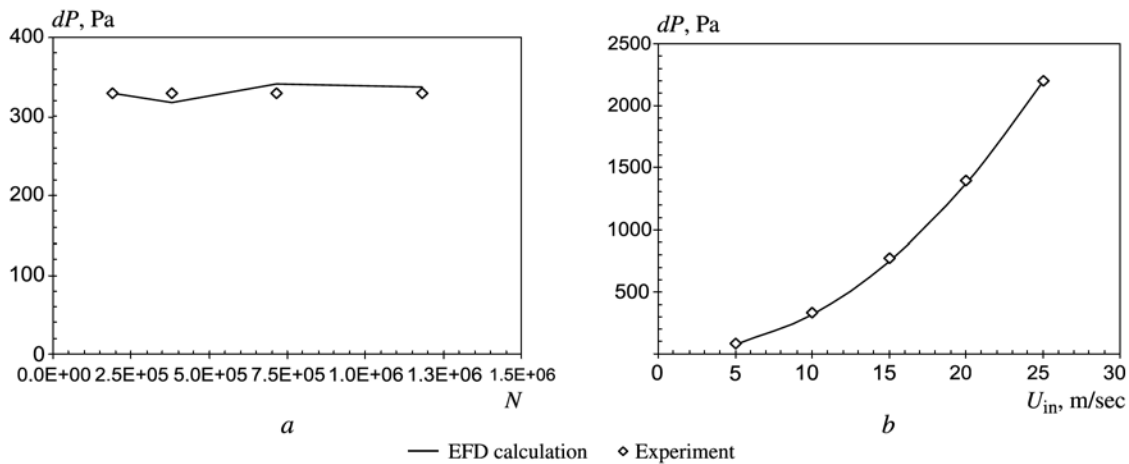


Fig. 3. Dependence of hydraulic resistance of Stairmand HE cyclone: *a*) on number of cells of computational mesh; *b*) on air velocity at cyclone inlet.

II. *Cyclone with a bin.* In contrast to the Stairmand HE cyclone, the experimental data for a cyclone with a bin are distinguished by a wide variety of conditions and temperatures and include evaluation of the operation efficiency [4]. The geometry of the cyclone is shown in Fig. 2. The key dimensions of the cyclone are given in Table 3 [4].

This cyclone differs from the Stairmand HE one in having a bin and a flow straightening device in the end part of the outlet pipe. This arrangement allows one to get almost a uniform flow at the outlet, thereby dispensing with the need for solving the problem in external formulation, i.e., a constant static pressure at the expulsion point, which is a fully correct boundary condition for internal formulation of the problem.

The dimensions of the calculation region are equal to the overall dimensions of the cyclone. The same approach was used for discretization of this region as was used for the Stairmand HE cyclone. A calculation mesh with 350,000 control volumes was used as the base for designing this cyclone. The same calculation methods and procedures were employed for pressure differential averaging as were employed for the Stairmand HE cyclone.

For sampling operation regimes, the cyclone efficiency was also assessed, i.e., the motion and settling of particles of various diameters were calculated. The density of the particulate material is taken as  $2650 \text{ kg/m}^3$ .

It was suggested that on the inner surfaces of the cyclone the particle repulsion condition is ideal. The inner surfaces of the bin are considered to be fully absorbing surfaces.

The inlet pipe discharged 500 particles of each diameter within the studied particle size range. Thereafter, the trajectory of each particle was calculated with due regard for the referred boundary conditions. The cyclone efficiency was determined as the ratio of the number of captured dust particles of each diameter to the total number of discharged particles of this diameter.

In the scientific and technical literature, a sceptical attitude developed with regard to the use of  $k$ - $\epsilon$  turbulence model and its modification for modeling of swirling flows, including in cyclones [5]. Without questioning the validity of such assessments for local characteristics, we shall try to demonstrate the usefulness of the  $k$ - $\epsilon$  model in engineering calculations of integral characteristics of cyclones.

We shall distinguish three methodological factors of successful application of  $k$ - $\epsilon$  turbulence model for calculation of flow in cyclones.

1. In the case of presence at the cyclone outlet a flow with a pronounced tangential component, the problem is recommended to be solved in external formulation. In the presence at the outlet of different kinds of flow straightening devices, this factor ceases to be important.

2. Requirements for the calculation mesh: inside the cyclone it is recommended to avoid cells with different subdivision levels; uniform subdivision level is preferable, especially in regions of highly vigorous swirling.

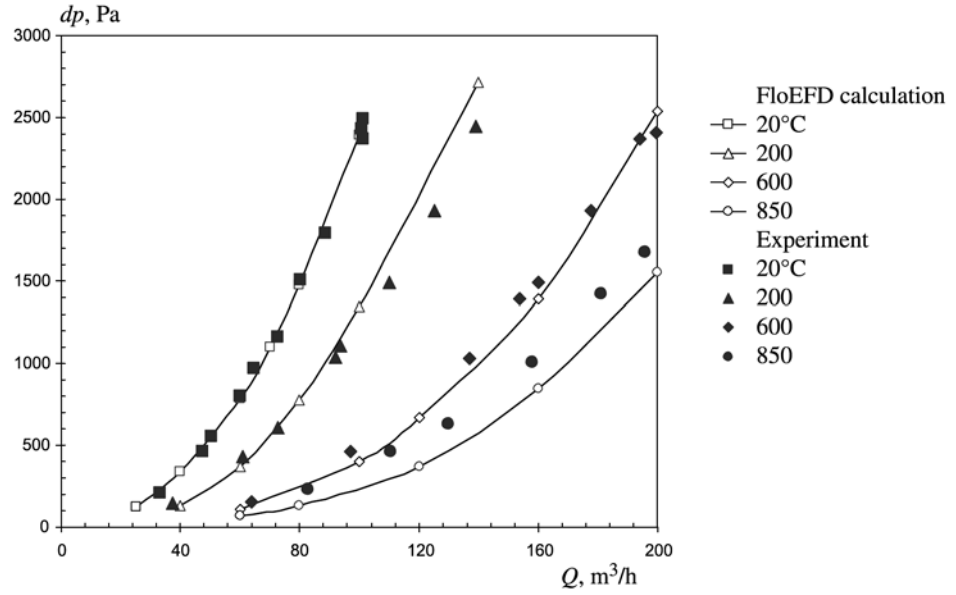


Fig. 5. Dependence of hydraulic resistance  $dP$  of cyclone with bin on throughput  $Q$  at various gas temperatures.

3. Unsteady calculation with a constant time step gives a more correct hydraulic resistance calculation result [6]. The length of the time step is a critically important factor for getting satisfactory result. Its value must not therefore exceed a certain critical value

$$\Delta t_{cr} = \frac{\min(D_d, D_{op})}{U_{max}} = \frac{\min(D_d, D_{op})}{U_{in} D_c} D_{op}, \quad (3)$$

where  $\Delta t_{cr}$  is the critical time step,  $D_d$  is the diameter of the dust expulsion hole,  $D_{op}$  is the diameter of the outlet pipe,  $U_{max}$  is the maximum air velocity in the cyclone,  $U_{in}$  is the air velocity at the inlet pipe entrance, and  $D_c$  is the diameter of the cylindrical part.

We do not claim universality of these methodological recommendations for all mathematical flow models and all algorithms for their realization. It is possible that these propositions are valid essentially for the FloEFD package. Nonetheless, they may be useful within the framework of other CFD packages as well.

The results of calculation of the hydraulic resistance of the Stairmand HE cyclone as a function of the number of cells of the computational mesh and the results of the physical experiment [3] are plotted in Fig. 3a. The time step was estimated in keeping with (3) and, for example, for entry velocity of 10 m/sec, it was taken as 0.005 sec. The number of iterations for attainment of quasisteady-state regime varied from 1000 to 2000 depending on the cyclone throughput. The calculations were found to be fairly accurate (within 5%), and the results were negligibly sensitive to variation of quantitative parameters of the computational mesh. A computational mesh with 380,000 cells was chosen as the base for all calculations of this cyclone.

The plot in Fig. 3b shows good calculation accuracy in the entire cyclone efficiency range, for which experimental data were obtained. The mean relative calculation error was 2–3% and the maximum, not more than 5%.

The results of calculation of airflow in the cyclone with a bin and the experimental data are added in Figs. 4–6. The time step was determined in keeping with (3) and, was taken as 0.0006 sec, for example, for the 80 m³/h volume airflow rate. The number of iterations for attainment of quasisteady-state regime varied from 2000 to 3000 depending on the throughput.

The typical view of the velocity field inside the cyclone is shown in Fig. 4. The results correspond to the following calculation case: throughput of the cyclone 80 m³/h, gas temperature 20°C, and physical process time 3 sec. The spatial structure inside the cyclone is noticeably intricate.

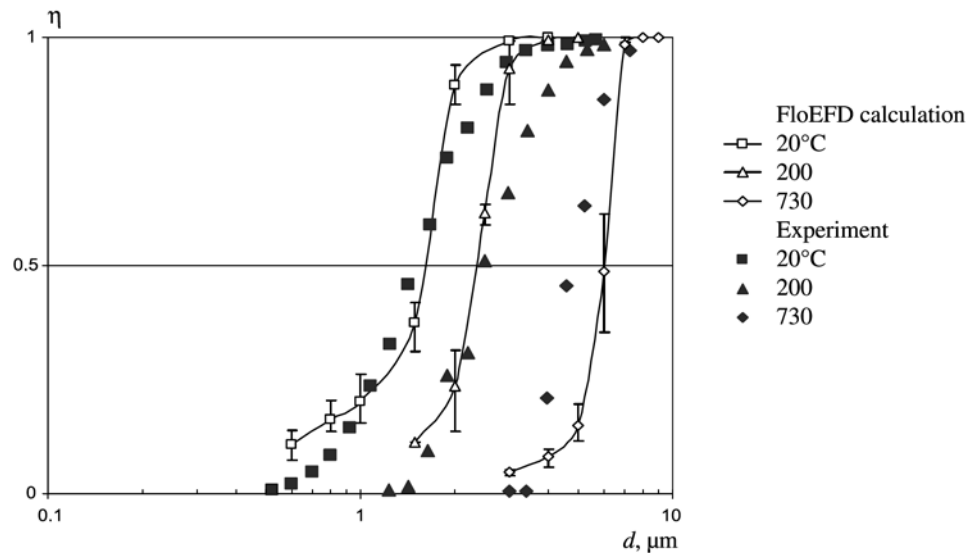


Fig. 6. Dependence of gas purification degree  $\eta$  on particle size at various gas temperatures at  $60 \text{ m}^3/\text{h}$  cyclone throughput.

In Fig. 5, the calculated pressure drops (gradients) are compared with the experimental data obtained at various gas temperatures at the inlet of the cyclone with a bin [4]. In practically the entire volume flow rate range, the calculated and experimental data show good agreement. The relative computation error in all the studied volume flow rate and temperature ranges is not more than 5–10%, and only for the high-temperature flows ( $t > 600^\circ\text{C}$ ) was the maximum error slightly above 10%.

Note that most cyclones are designed for purification of gas flows whose temperature is rarely above  $400^\circ\text{C}$ . So, temperatures above  $400^\circ\text{C}$  may be taken as extreme, but even under such conditions the described mathematical model and algorithms of its realization in FloEFD showed fully satisfactory results, and, moreover, within the framework of a single approach without special corrections for gas temperature at the cyclone entrance.

The calculated gas purification degrees at various temperatures are shown in Fig. 6. Since the flow pattern in a cyclone is unsteady, the probability of particle precipitation for each diameter was calculated by averaging the results of five discharges of particles. Each particle discharge was based on frozen airflow field in the cyclone that was obtained at different points of time. The vertical bars at each calculation point correspond to maximum and minimum probability of precipitation of a particle with a definite diameter obtained in a series of five particle discharges.

The average gas purification degree calculation accuracy is found to be satisfactory relative to the experimental data [4]. Note that the calculated quantity  $d_{50}$  (diameter of particles settled under actual conditions of cyclone operation with an efficiency of 50%) exactly reproduces the experimental values, especially at gas temperatures below  $200^\circ\text{C}$ . At higher temperatures, the calculation accuracy decreases a little. The calculated cyclone efficiency curves have a slightly steeper gradient relative to the experimental (Fig. 6).

### Conclusions

1) The proposed mathematical model and its numerical actualization using modern numerical modeling software package, FloEFD for instance, allows one to adequately calculate the hydraulic resistance and operational efficiency of air cyclones at various feed-air temperatures in a wide gas load range.

2) The proposed solving procedure may be useful for engineering calculations of integral aerodynamic characteristics of technical devices involving vigorously swirling working fluid flows, including within the framework of modified  $k-\epsilon$  turbulence model.

3) Use of FloEFD computing package for solving the referred type of problems entails moderate computing costs, which, in combination with full integration of the package over all leading CAD systems allows significant shortening of the equipment designing and optimization cycle time.

## REFERENCES

1. *Enhanced Turbulence Modeling in FloEFD<sup>TM</sup>*, MGC 02-11, TECH9670-w, Mentor Graphics Corporation (2011).
2. C. B. Henderson, "Drag coefficients of spheres in continuum and rarefied flows," *AIAA J.*, **14**, No. 6, 707–708 (1976).
3. W. D. Griffiths and F. Boysan, "Computational fluid dynamics (CFD) and empirical modeling of the performance of a number of cyclone samplers," *J. Aerosol Sci.*, **27**, No. 2, 281–304 (1996).
4. T. Lorenz, "Heißgas Entstaubung mit Zyklonen," *VDI Fortschritt Berichte, Reihe 3, Verfahrenstechnik*, No. 366, VDI-Verlag, Dusseldorf (1994).
5. F. Boysan, W. H. Ayer, and J. A. Swithenbank, "Fundamental mathematical modeling approach to cyclone design," *Trans. Inst. Chem. Eng.*, **60**, No. 4, 222–230 (1982).
6. C. A. Montavon, H. Grotjans, I. S. Hamill, et al., "Mathematical modeling and experimental validation of flow in a cyclone," *BHR Int. Conf. Cyclone Technol. No. 5*, May 31 – June 2, 2000, Warwick, pp. 175–185.